ENGINEERING INTERMEDIATE BAND MATERIALS BASED ON METAL-DOPED CHALCOGENIDE COMPOUNDS BY QUANTUM MECHANICAL CALCULATIONS

P. Wahnón , P. Palacios , K. Sánchez , I. Aguilera and J.C. Conesa

ABSTRACT: In this work we present Density Functional Theory calculations (at the standard theory level and beyond) for metal-containing chalcogenide compounds derived from the chalcopyrite $CuGaS_2$ and the spinel $MgIn_2S_4$. The purpose of the work is to develop a material which can be used to create a more efficient photovoltaic solar cell. This material must have a partially filled band inside the band-gap of an appropriate host semiconductor.

For chalcopyrite alloy materials we have previously made ab-initio calculations using the Density Functional formalism in the Generalized Gradient Approach for different metals as Ti, V, Cr, and Mn substituting for Ga. For the Ti and Chromium cases, the observation of an intermediate band seems promising, so we have made now further calculations using two more advanced methods which handle more accurately the electron correlation and exchange effects. For Indium thiospinel materials with Vanadium as susbtituent we present here the first standard DFT calculations, showing that this compound is also a good intermediate band material candidate.
Keywords: Chalcopyrite, Fundamental, ab-initio

1 INTRODUCTION

In the search for more efficient solar cells our group proposed recently, on the basis of quantum mechanical Density Functional Theory (DFT) studies, novel materials to implement the intermediate band (IB) concept, which has been postulated to be able to enhance the efficiency of photovoltaic (PV) cells. With such IB, besides the normal electron excitation from the valence band (VB) to the conduction band (CB) one can have also two excitations of lower energy from the VB to the IB and from the IB to the CB, allowing to use a larger fraction of the solar spectrum and to obtain an increase in photocurrent without decreasing the photovoltage [1]. This IB concept leads to an ideal solar energy conversion efficiency limit of up to 63.2% at maximum concentration. To realise it, the IB (which should not be a discrete level) must be partially filled and isolated in energy from the ordinary VB and CB of the host semiconductor; these requirements must be fulfilled in order to have an efficient charge separation and good absorption coefficients and quantum efficiencies.

In the materials proposed by us, a partially filled IB is formed inside the band-gap of an appropriate III-V semiconductor [2 and references therein] or of an I-III-VI_2 semiconductor [3, 4] by partial substitution of the III-type atoms with some properly chosen transition metal atoms. The energetics of these substitutions were studied, using also quantum mechanical DFT calculations, to ascertain the practical feasibility of formation of these IB materials [4, 5]. In those works we have calculated electronic structures for these materials using as substituents 3d metal elements like Titanium, Vanadium, Chromium and Manganese at different dilution levels, and interpreted the effects of this substitution considering that the metal is in a M^{3+} redox state and the 3d states are partially filled and splitted in two manifolds as corresponds to the tetrahedral environment of the metal.

In those first theoretical calculations we used DFT at the local density approximation (LDA) and the generalized gradient approximation (GGA) levels including spin polarization. The calculations at these levels underestimate band-gap widths and localization effects; therefore in cases where the IB formation seems to be clear in this type of materials we have used two more advanced approaches: the DFT+U method, which add a Hubbard term to the calculations, and the Exact-Exchange method (EXX), which improves the exchange term that is not handled accurately in standard DFT.

In this paper we first present DFT calculations for the host semiconductor of this type of materials and with transition metal substitution.

2 MODELS

2.1 Chalcopyrite type materials

I-III-VI_2 type chalcopyrite semiconductors crystallize in the space group I-42d, number 122, with four formula units in each tetragonal centered unit cell. It is a superstructure of zinc-blende, distorted in the z direction, where each atom is tetrahedrally coordinated to four neighboring atoms. The unit vectors of the chalcopyrite primitive cell are (a,0,0), (0,a,0), (a/2,a/2,c/2). The cations are located at 4a and 4b Wyckoff positions while anions are located at 8d.

The unit cell used to model the substituted chalcopyrite alloy has been constructed from the vectors (a,b,c) of the tetragonal chalcopyrite cell according to a'=(a+b+c)/2, b'=(a+b-c)/2 and c'=b-a. The resulting structure has 16 atoms in this unit cell with one Gallium atom replaced by a transition metal (M). This $Cu_4Ga_3S_8M$ system (12.5% in Metal) is the primitive of a centered monoclinic lattice which has C2 symmetry. We have also studied more diluted system as the $Cu_8Ga_7S_{16}M$ (6.25 % in Metal) as shown in Fig. 1.

2.2 Spinel type materials

II-III_2-VI_4 spinel semiconductors crystallize in the cubic space group Fd-3m, number 227, with eight formula units per face-centered cubic cell. In this structure the anions form a fcc lattice, in which the octahedral and tetrahedral interstitial sites (8a and 16d Wyckoff positions) are occupied respectively by 2/3 and 1/3 of the cations.

We have studied the $MgIn_2S_4$ system with the direct spinel structure where the Indium occupies the octahedral sites and the Magnesium the tetrahedral sites, although it is known that some degree of inversion (permutation of both metals between these sites) may exist [6]. For the spinel derivative we have substituted by a transition metal one fourth of the Indium atoms. We finally obtained a $Mg_2MIn_3S_8$ structure as shown in Fig. 1.

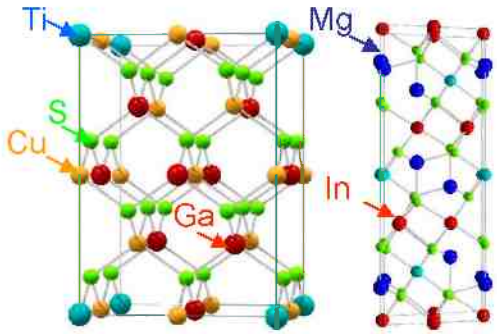

Figure 1: Structures of the substituted materials $Cu_8Ga_6S_{16}M$ chalcopyrite (left) and $Mg_2In_3S_8M$ spinel (right). The light blue balls represent M = Ti, V or Cr.

3 METHODS

3.1 Standard DFT calculations

We have carried out spin-polarized electronic structure DFT calculations at the GGA Perdew and Wang functional (PW91) level using the plane-wave VASP code with ultrasoft potentials [7] and a plane wave basis set with an energy cutoff of 233.7 eV for the chalcopyrite type and 211 eV for the spinel type materials. The Brillouin zone was sampled using 6x6x6 Monkhorst-Pack grids with 112 irreducible k-points including the Gamma point in the calculations. We have relaxed the ions and the cell until convergences of 0.01 eV/Ang for the forces and 10E-5 for the self-consistent field cycles. The atomic radii used for the projected density of states were 1.60, 1.27, 1.66 and 1.34 Ang for Mg, In, S and V respectively.

3.2 More advanced calculations; beyond DFT

Standard DFT has a known problem in predicting band-gaps in semiconductors because it takes into account the exchange interaction in an inadequate way. In order to obtain better band-gap results, more accurate calculations beyond standard DFT have been made for the parent and the substitute chalcopyrite using the EXX method as implemented by us in the DFT code SIESTA, using an atomic basis functions representation [8]. This method, taking into account the electron exchange interaction more precisely than standard DFT, was used successfully in III-V semiconductors and their metal-doped variants [9]. In these calculations electron correlation is not considered.

The effect of electronic correlation is also not well reproduced by standard DFT, especially when partially filled 3d levels are present. To improve the prediction accuracy we have made GGA+U calculations, which include an effective on-site Coulomb parameter U (a Hubbard term). In this work the value of U has been taken from similar cases in the literature [10,11] although we are also making calculations to obtain it using ab-initio methods [12].

4 RESULTS

4.1 $CuGaS_2$ chalcopyrite

In order to validate our ab-initio calculations for the substituted systems, we have studied first the host semiconductor $CuGaS_2$ to compare the results with experimental data. A band gap width of ca. 1 eV is obtained; this is lower, as expected for a standard DFT result, than the 2.4 eV value experimentally known for this compound [13], and can be compared with the similar values obtained in other theoretical works [14]. However, the lattice parameter 5.34 Ang found after geometry relaxation do compare very well with experimental data [15].

Using the EXX method, we obtain for the chalcopyrite band-gap a value E_g=1.8 eV, closer to the experiment than that given by the GGA calculation. In Fig. 2 we compare these EXX results with those of the GGA calculation, showing this band gap increase. As expected, the better treatment of the electronic exchange potential leads to an increased separation between the filled and empty levels.

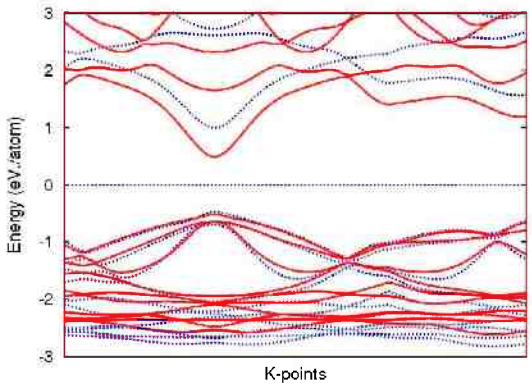

Figure 2: $CuGaS_2$ band diagrams as obtained with GGA (red solid line) and EXX (blue dashed line)

4.2 Chalcopyrite type alloys $(Cu_4Ga_3S_8)M$

Results for these Metal substituted compounds were obtained after geometry relaxation. It is found that the local geometry around the Metal is only slightly distorted from the initial tetrahedral one.

For the metal-substituted compounds the results are strongly spin-polarized. At GGA-level we only show here results for the Ti-substituted system, but we have also made calculations for the Cr, V and Mn cases. In the case of Ti, for the majority spin curve a relatively narrow band with two levels, which are due to d-type titanium-centered orbitals, appears crossing the Fermi level (Fig. 3). The conduction band can be interpreted as formed by the CB of $CuGaS_2$ plus three more empty 3d levels due to Titanium. We found a small overlap between this new Titanium band and the CB. For the minority spin the Titanium-derived states (all of them empty) are located at higher energy, overlapping with the CB states. For these systems, if we reduce the concentration of the transition metal (using a $Cu_8Ga_7S_{16}M$ cell) the electronic structure is qualitatively unaltered. Only a small decrease in the IB width is found, but the corresponding levels still have a delocalised band character so we still expect to have an efficient IB behavior.

EXX calculations have been carried out for this Titanium alloy system, and observed in them that the overlap previously shown to appear in GGA calculations between the CB and the metal-derived band has now disappeared, thanks to the above mentioned higher separation between VB and CB. Moreover we notice that the relative positions of the VB and the IB has not changed from that previously obtained by the standard DFT calculation. In Figs. 3 and 4 we present the comparison between the standard DFT-GGA and the DFT-EXX. In the EXX calculations the (majority spin) band due to Titanium appears (blue line) well within the forbidden band; an IB well isolated within the gap has thus been obtained. In the minority spin curves an increase in the gap over the GGA result is observed.

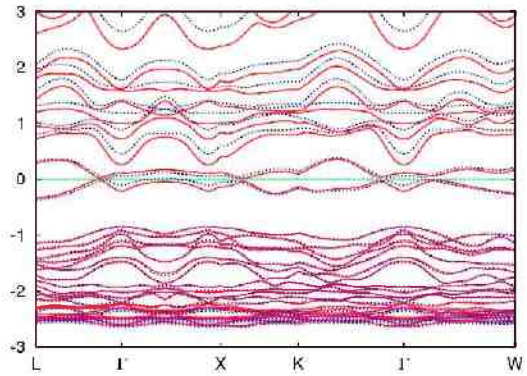

Figure 3: GGA (red solid line) and EXX (blue dashed line) results for the $Cu_4Ga_3S_8Ti$ majority spin band diagrams.

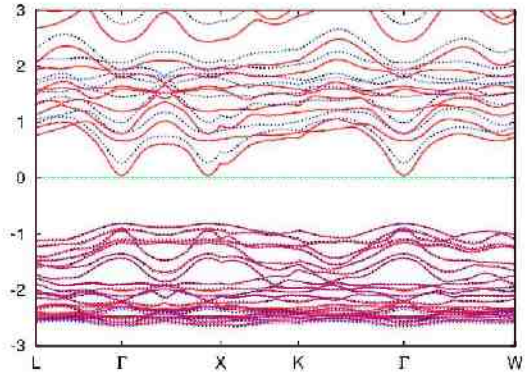

Figure 4: GGA (red solid line) and EXX (blue dashed line) result for the $Cu_4Ga_3S_8Ti$ minority spin band diagrams.

GGA+U calculations were also carried out, studying the effect of a better treatment of the electronic correlation on the results obtained for the substituted systems and trying to improve the prediction accuracy. The considered substituents were Titanium and also Chromium, since GGA level calculations (not presented here; see [4]) suggested it might be as good as Titanium for producing an adequate IB. The values for the Hubbard term U were taken from the literature (2.0 eV and 5.0 eV for Ti and Cr respectively).

The GGA+U results show a lowering in energy of the filled 3d electron states and a rise in the empty states. For Titanium we clearly obtain a splitting of the metal bands, leaving a one-electron filled majority spin IB separated from the CB and the VB, while for Chromium the filled metal states overlap the VB. Therefore, according to this more accurate calculation the Chromium system will not be valid for realizing the IB concept. In Fig. 5 we show the density of states curves for Ti (red solid line) and Cr (blue dots) substituted $CuGaS_2$ systems obtained at the GGA+U level.

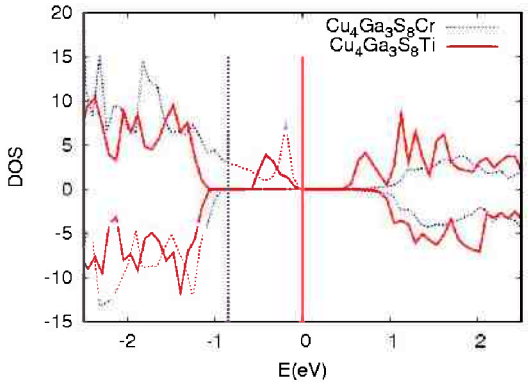

Figure 5: Density of states curves computed at the GGA+U level for Ti-(red solid line) and Cr-doped (blue dotted line) $CuGaS_2$. Vertical lines mark the Fermi level for each system.

4.3 $MgIn_2S_4$

As made for the chalcopyrite systems, in order to validate the results for the substituted systems, we have made first calculations for the experimentally known $MgIn_2S_4$ (assuming it to be a fully direct spinel). After geometry relaxation the anion positions compare very well with other theoretical calculations for this system [16]. The experimental cell parameter 10.71 Ang [17] shows an increase of 0.07Angs in our GGA calculation. A band gap width of ca. 1.65 eV is observed theoretically; this is lower than the experimental value of 2.1eV [18], but the difference is smaller than that found for the $CuGaS_2$ chalcopyrite and also smaller than in other theoretical results published for this system [16]. The GGA-obtained total and projected density of states for this material is shown in Fig. 6.

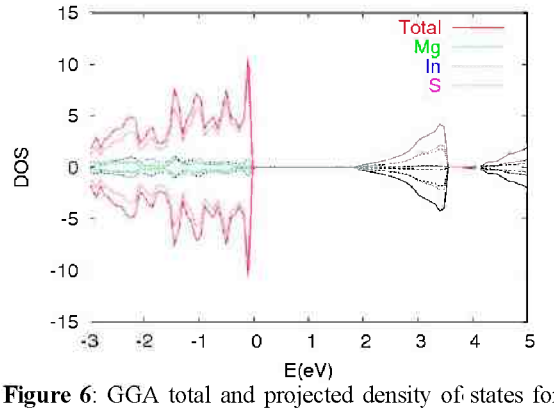

Figure 6: GGA total and projected density of states for the $MgIn_2S_4$ system.

4.4 Spinel type alloys $(Mg_2In_3S_8)M$

One Indium atom is replaced by a Metal in the $Mg_2In_4S_8$ system. As the Indium has an octahedral environment of sulphurs, the splitting of the 3d metal

levels is different to that appearing in the chalcopyrite substitutions where the III-type atoms environment is tetrahedral. So the lower energy 3d levels constitute now a three level branch, not a two-level branch as in the chalcopyrite case. For this reason Vanadium substitution, which in the chalcopyrite was not interesting for the IB concept since that branch would be fully occupied (and furthermore turns out to overlap the valence band), can now produce a partially filled IB. This is also still true for Titanium, but no longer for Chromium.

After geometry relaxation, as in the chalcopyrite cases, the local geometry around the metal presents only a slight distortion from the initial octahedral environment for these systems. In Fig. 7 we show the total DOS (red solid line) and atom projected DOS (dashed lines) for the Vanadium substituted system. In the atom projected curve it is clearly shown that the new levels forming a clear IB come from the vanadium 3d orbitals. In this system, the Fermi level crosses the IB, which is partially filled with two electrons and fulfills the desired IB requirements; it has been thus proposed for use in efficient photovoltaic systems [19].

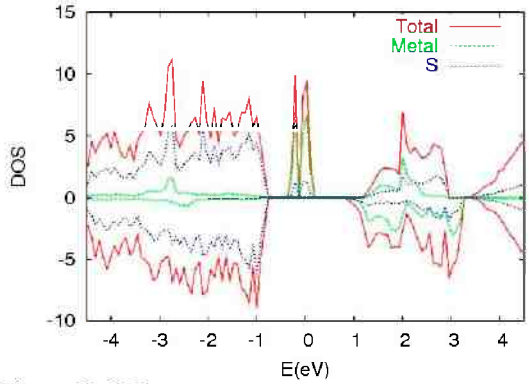

Figure 7: GGA total and projected density of states for the $Mg_2In_3S_8V$ system.

5 CONCLUSIONS

We have made ab-initio electronic structure calculations for $CuGaS_2$ and $MgIn_2S_4$ systems with the III type atom (Gallium or Indium) partially substituted by a transition metal (Ti, V or Cr). Some of these systems seem to be promising materials to realize the intermediate band solar cell concept. The calculations have been made using standard DFT methods, as the GGA, and more accurate ones as the GGA+U and EXX approaches. According to the results of these latter, a Titanium substituted chalcopyrite system seems to fulfill the intermediate band requirements. For the spinel type materials the Vanadium transition metal substitution at the octahedral indium site leads also to an isolated intermediate band and is a good candidate for application in photovoltaics.

ACKNOWLEDGEMENTES

We would like to acknowledge the funding from project FULLSPECTRUM (contract. SES-CT-2003-502620) of the 6th European Framework Programme and the from the CALIBAND (MAT2006-10618) project of the Spanish Ministry of Education and Science and from the Community of Madrid NUMANCIA-MA(S-05050/ENE/0310) Research Programme.

REFERENCES

[1] A. Luque, A. Marti, Phys. Rev. Lett. 78 (1997) 5014.
[2] P. Palacios, J. J. Fernández, K. Sánchez, J.C. Conesa, P. Wahnón, Phys. Rev. B 73 (2006) 085206.
[3] P. Palacios, K. Sánchez, J.C. Conesa, P. Wahnón, Phys. Stat. Solidi (a) 203 (2006) 1395.
[4] P. Palacios,K. Sánchez, J.C. Conesa, J.J. Fernández, P. Wahnón, Thin Solid Films 515 (2007) 6280
[5] P. Palacios, P. Wahnón, S. Pizzinato, J.C. Conesa, J. Chem. Phys. 124 (2006) 014711
[6] M. Wakaki, O. Shintani, T. Ogawa, T. Arai, Jpn. J. Appl. Phys., 21 (1982) 958
[7] G. Kresse, J. Hafner, Phys. Rev. B 47 (1993) RC558; G. Kresse, J. Furthmüller, Phys. Rev. B 54 (1996) 11169, G. Kresse, J. Hafner, J. Phys.: Condens. Matter 6 (1994) , 8245.
[8] J. J. Fernández, C. Tablero, P. Wahnón, Int. J. Quantum Chem., 91 (2003) 157
[9] J.J. Fernández, C. Tablero and P. Wahnón, Comput. Mater. Sci. 28 (2006) 2774
[10] A.I. Liechtenstein, V.I. Anisimov, J. Zaanen, Phys. Rev. B 52 (1995) R5467.
[11] A.I. Poteryaev, A.I. Lichenstein, G. Kotliar, Phys. Rev. Letters 93 (2004) 086401.
[12] M. Cococcioni, S. Gironcoli, Phys. Rev. B, 71 (2005) 035105.
[13] S. Shirakata, K. Murakami, H. Kukimoto, Jpn. J. Appl. Phys. Part 1 **28**, 1728 (1989).
[14] S. Picozzi, Y.J. Zhao, A.J. Freeman, B. Delley, Phys. Rev. B **66,** 205206 (2002); J.E. Jaffe, A. Zunger, Phys. Rev. B **28**, 5822 (1983).
[15] H. Hahn, G. Frank, W. Klinger, G. Storger, Z. Anorg. Chem. 271 (1983) 153; H. W. Spiess, U. Haeberlen, G. Brandt, A. Rauber, J. Schneider, Phys.Stat. Solid. B 62 (1974) 183. S.C. Abrahams, J.L. Bernstein, J. Chem. Phys. 59 (1973) 5415.
[16] M. Marinelli, S. Baroni, F. Meloni, Phys. Rev. B, 38 (1988) 8258
[17] L. Gastaldi, L. Lapiccierlla, J. Solid. State. Chem. 30 (1979) 223
[18] P. M. Sirimanne, N. Sonoyama, T. Sakata, J. Solid State Chem., 154 (2000) 476
[19] Filed Spanish patent application. Ref. nr. ES 200702008. Prioritiy date: July 19th 2007